Received: 19 October 2022 | Revised: 7 February 2023 | Accepted: 22 February 2023

DOI: 10.1002/mgg3.2162

Molecular Genetics & Genomic Medicine Open Access WILEY

ORIGINAL ARTICLE

Large heterozygous deletion and uniparental disomy masquerading as homozygosity in *CHKB* gene

Tenghui Wu[1,2] | **Ciliu Zhang**[1,2] | **Fang He**[1,2] | **Li Yang**[1,2] | **Fei Yin**[1,2] | **Jing Peng**[1,2]

[1]Department of Pediatrics, Xiangya Hospital of Central South University, Changsha, China

[2]Clinical Research Center for Children Neurodevelopmental disabilities of Hunan Province, Xiangya Hospital of Central South University, Changsha, China

Correspondence
Jing Peng, Department of Pediatrics, Xiangya Hospital of Central South University, 87 Xiangya Road, Changsha, Hunan Province, China.
Email: pengjing627@126.com

Funding information
National Natural Science Foundation of China, Grant/Award Number: 82071462

Abstract

Background: *CHKB* mutations have been described in 49 patients with megaconial congenital muscular dystrophy, which is a rare autosomal recessive disorder, of which 40 patients showed homozygosity.

Methods: Peripheral blood genomic DNA samples were extracted from patients and their parents and were tested by whole exome sequencing. Quantitative PCR was performed to detect deletion. Single nucleotide polymorphism analysis was performed to identify uniparental disomy. Quantitative PCR and western blot were used to measure the expression level of *CHKB* in patient 1-derived immortalized lymphocytes. Mitochondria were observed in lymphocytes by electron microscopy.

Results: Two unrelated cases born to non-consanguineous parents were diagnosed with megaconial congenital muscular dystrophy due to apparently homozygous mutations (patient 1: c.225-2A>T; patient 2: c.701C>T) in the *CHKB* gene using whole exome sequencing. Quantitative PCR revealed that patient 1 had a large deletion encompassing the *CHKB* gene, inherited from the mother. Single nucleotide polymorphism analysis revealed patient 2 had paternal uniparental isodisomy containing the *CHKB* gene. In the immortalized lymphocytes from patient 1, decreased expression of *CHKB* was revealed by quantitative PCR and western blot, and giant mitochondria were observed using electron microscopy.

Conclusion: We provide a possibility to detect giant mitochondria in other cells when muscle was not available. Moreover, clinicians should be aware that homozygous variants can be masqueraded by uniparental disomy or large deletions in offspring of non-consanguineous parents, and excessive homozygosity may be misdiagnosed.

KEYWORDS

CHKB, large deletions, megaconial congenital muscular dystrophy, uniparental disomy

1 | INTRODUCTION

Megaconial congenital muscular dystrophies (CMDs) caused by mutations in the *CHKB* (OMIM: 612395) gene with autosomal recessive inheritance are characterized by early-onset muscle weakness and profound intellectual disability, increased levels of serum creatine kinase (CK), and giant mitochondria in skeletal muscle biopsies (Chan et al., 2020). The *CHKB* gene spans 11 exons and encodes the choline kinase, which catalyzes choline phosphorylation by ATP in the presence of Mg^{2+}, yielding phosphocholine and ADP (Ishidate, 1997). *CHKB* gene mutations clustering in all exons leads to choline kinase deficiencies.

CHKB mutations have been described in 49 patients with megaconial CMD, of which 40 patients showed homozygosity. Herein, we report two Chinese patients with megaconial CMD carrying apparently homozygous variants. Our two families are unique in that they show discordant segregation that only a single parent was found to harbor the same heterozygous variant. In this study, the potential molecular etiologies of two patients were further investigated, and the reason of high percentage of homozygosity in *CHKB* gene was summarized. Combination of genetic test and muscle biopsy is an effective diagnosis means for megaconial CMD. As an invasive method, muscle biopsy is not always accepted by patients and their parents, especially when the patients show a mild phenotype. In this study, we first try to detect the size and morphology of mitochondria in immortalized lymphocytes using electron microscopy.

2 | METHODS

2.1 | Clinical data collection and ethical compliance

The clinical and genetic materials were retrospectively analyzed. The research protocol has been approved by the ethics committee of Xiangya Hospital of Central South University. An informed consent for the gene sequencing and the publication of the results was signed by the guardian of patient.

2.2 | Genetic tests

Genomic DNA (gDNA) samples were extracted from peripheral blood that was collected from the patients and their parents. The whole exome sequencing was performed on Illumina novaseq platform with at least Q20 base quality, and >30× mean nuclear coverage. Sequences were compared to the human reference genome GRCh38/HG38 using the NextGENe software (SoftGenetics) for true and false variants identification. Bam files were locally re-compared using GATK series software. Annovar was used to annotate VCF variation files. Principles for screening pathogenic mutation: (1) to screen out exon region mutation and non-synonymous mutation. (2) to screen out variants not observed or less than 5% in ExAC_EAS, ExAC_ALL, 1000Genomes, gnomAD databases. (3) to evaluate variants according to dbSNP, OMIM, HGMD, ClinVar and other databases. (4) to predict the protein function by SIFT, Polyphen2, MutationTaster and other protein function prediction software. Pathogenic variants were screened according to ACMG classification guidelines and patients' clinical phenotypes. Genotyping with single nucleotide polymorphisms (SNPs) and polymorphic microsatellite markers was performed.

The copy number variation (CNV) sequencing was performed as previously described, by random fragmentation and short read sequencing using the Illumina NextSeq500 sequencer (Illumina). The resolution was 25–100 kb. Sequencing reads were cleaned by removing the read when a base quality was less than Q20 and mapped to the reference human genome version GRCh38/hg38. The high variation regions indicating highly homologous or repeated regions across different samples were excluded for further analysis. The interpretation of copy number variations (CNVs) was based on the Database of Genomic Variants DGV, DECIPHER, OMIM and peer-reviewed literature.

2.3 | Quantitative real-time PCR for DNA

Presumed *CHKB* deletions were validated using quantitative real-time PCR (qPCR) on gDNA with primers specific to sequences inside the *CHKB* gene (GRCh38/hg38, probe 1: Chr22:50579314–50579522; probe 2: Chr22:50579870–50580070; probe 3: Chr22:50581322–50581528). The amplification was normalized to the RPN2 reference gene (Chr20:37237635–37237740). The amplification was performed in a qPCR system (SLAN-96P) using the SYBR Green methods. The standard thermocycling program: 95°C for 3 min, 40 cycles of 94°C for 15 s, 60°C for 40 s followed by a melting curve. Relative changes in genomic sequence abundance were calculated using the $2^{(-\Delta\Delta CT)}$ method.

2.4 | Construction and culture of immortalized lymphocytes

Immortalized lymphocytes were derived from peripheral blood mononuclear cells obtained from 5 mL heparin

sodium-treated blood. It takes about one month to construct immortalized lymphocytes as previously described (Wu et al., 2022). Immortalized lymphocytes were cultured in RPMI 1640 medium (Thermo Fisher Scientific) supplemented with 10% fetal bovine serum (Sigma-Aldrich), 1% Antibiotic-Antimycotic (Thermo Fisher Scientific).

2.5 | Quantitative real-time PCR for RNA

Total RNA was extracted as previously described (Chomczynski & Sacchi, 2006). Random 6-mer primers (Vazyme) were used for reverse-transcription. The qPCR was performed using primers targeted to *CHKB* and β-actin mRNA on a StepOne Real-Time PCR System (Thermo Fisher Scientific) by using ChamQ Universal SYBR qPCR Master Mix (Vazyme). Primers: *CHKB* F/*CHKB* R: GGACCATGGAGCGGTACCTA/ACTTCCTGAGGTTG CCCATC; β-actin F/β-actin R: GACCTGTACGCCAA CACAGT/AGTACTTGCGCTCAGGAGGA. Data were analyzed using the 2(−ΔΔCT) method.

2.6 | Western blot

Total proteins were extracted from whole cells using the RIPA lysis buffer (Beyotime Biotchnology). Proteins were separated using 10% sodium dodecyl sulfate-PAGE and transferred on to 0.45 μm polyvinylidene difluoride membrane (MilliporeSigma™ IPVH00010). Proteins were probed with Anti-ChoKB Antibody (1:500, ER63004, HuaAn), Anti-Cytochrome C Antibody (1:5000, ab133504, Abcam), and then incubated with a HRP Conjugated AffiniPure Goat Anti Rabbit IgG secondary antibody (1:5000, Boster Biological Technology). Signals were detected with chemiluminescent Imaging and Analysis System (MiniChemi). Integrated optical density quantification was performed using ImageJ.

2.7 | Transmission electron microscopy

The cells, cultured in a 25cm^2 cell culture flask (707003, NEST) with 15 mL culture medium, were collected by centrifugating at 129 *g* for 5 min (Eppendorf, Centrifuge 5810 R). Following fixation with 2.5% glutaraldehyde, the samples were embedded in agar and postfixed in 1% osmium tetroxide for 2 h at room temperature, washed, then dehydrated using a gradient series of ethyl alcohol and two acetone baths. Samples were then embedded in Embed 812 resin (SPI, 90529-77-4) and acetone solutions followed by embedding in embedding resin for 48 h. The blocks were sectioned transversely at 60–80 nm using a diamond knife (Daitome, Ultra 45°). Ultrathin sections were stained with 2% uranyl acetate and lead citrate for 15 min, and then photographed with a transmission electron microscope (acceleration voltage: 80 kV, high contrast mode, magnification: ×1.5 k and ×5 k; HT7700, Hitachi). All images were photographed under the blind. The number of mitochondria per cell and the length of the mitochondrial axis (including longitudinal sections and cross sections) were measured using the software ImageJ. Typical size and morphology of mitochondria were evaluated.

3 | RESULTS

3.1 | Clinical presentation

3.1.1 | Patient 1

A two-year-old girl, the first child of healthy non-consanguineous Chinese parents, was born by spontaneous vaginal delivery after an uneventful pregnancy. She could sit unsupported at 12 months, walk without support at 20 months, and speak at 23 months. At four years of age, she still had not acquired the ability to run, hop or jump and had difficulty climbing stairs and standing up. She was short in stature, weighed 11 kg (<3rd), and was 82 cm (<3rd) tall with a head circumference of 44 cm (<3rd). Decreased muscle strength and tension were noted. Her serum CK level was mildly increased (480 U/L, normal range 50–310 U/L). Electromyography (EMG) demonstrated typical myogenic damage. Brain magnetic resonance imaging (MRI) plain scan, electrocardiogram, and echocardiography were normal.

3.1.2 | Patient 2

A 14-year-old boy, the first child of healthy non-consanguineous Chinese parents, he showed poor exercise tolerance, could not run, and had difficulty climbing stairs. He required learning support at school, and attention deficit hyperactivity disorder was noted. More significant learning difficulties became apparent in junior high school. He was able to walk without support at 14 months and speak at 18 months. On examination at 14 years, he weighed 30 kg (<−3rd) and measured 150 cm (<10th) tall with muscle weakness and depressed deep tendon reflexes. His serum CK levels were significantly increased (1646 U/L, normal range 50–310 U/L). EMG demonstrated myogenic damage. Brain and muscle MRI plain and fluid-attenuated inversion recovery scan, electrocardiogram, echocardiography, and Aberrant Behavior Checklist for scaling in autism were normal.

3.2 | Genomic analysis

3.2.1 | Patient 1

The MLPA assay for detecting DMD mutations and CNV sequencing were normal. A homozygous splice variant was identified in the *CHKB* gene (NM_005198.4) by WES, which was confirmed by Sanger sequencing (Figure 1a). The splice variant was inherited from her father, but was not observed in her mother. Detailed sequencing data, including sequencing depth, is shown in Table 1. The biological relationship between the patient and her parents was confirmed. Next, qPCR was used to analyze the deletion that may overlap the c.225-2A>T variants to determine whether large deletions existed on another chromosome. As revealed in Figure 1b, the quantity of *CHKB* gDNA in the patient and her mother was half that of the normal control and her father. The patient had a maternal heterozygous deletion involving the *CHKB* gene.

3.2.2 | Patient 2

WES revealed a homozygous missense variant in *CHKB*, c.701C>T (p.Ser234Leu), which was inherited from her father, but was not observed in her mother (Figure 2a). Detailed sequencing data including sequencing depth are shown in Table 1. The difference is that segmental paternal uniparental disomy (UPD) in chromosome 22 containing *CHKB* gene, was confirmed according to the comparison of parental genotyping with SNPs and polymorphic microsatellite markers (Figure 2b). In addition, Compound heterozygous mutations were also identified in the *TTN* gene (NM_001267550.2: c.73517G>A, c.52687delA). However, c.73517G>A has been reported as "likely benign" or "benign" in ClinVar. Moreover, almost all these features can be explained by the *CHKB* variant, c.701C>T, which has been reported as "pathogenic" in megaconial CMD.

3.3 | CHKB expression levels

CHKB mRNA level of the patient 1 was determined via qPCR and showed a 75% reduction compared to the level in the healthy control ($p < 0.0001$) (Figure 1c). Western blot showed that CHKB protein level was significantly reduced in patient 1-derived immortalized lymphocytes (Figure 1d).

3.4 | Transmission electron microscopy

No significant difference for mitochondria number per cell was observed (Figure 1e). Violin Plot of mitochondrial diameter showed that the overall shape and distribution of tips were similar in both groups, but there were more outliers in patient 1 (Figure 1f). A longitudinally cut mitochondrion measured up to 3 μm in length, and these mitochondria had a more bright and swollen aspect with ruptured-like cristae compared to the healthy control (Figure 1g).

4 | DISCUSSION

A false interpretation of homozygosity for pathogenic variants in autosomal recessive disorders can lead to improper genetic counseling. Our study highlights the significance of comprehensive analysis to distinguish real homozygosity from presumed homozygosity in non-consanguineous families.

In this study, we identified the etiologies of presumed homozygous disease-causing variants of the *CHKB* gene in two patients. For patient 1, the c.225-2A>T was apparently homozygous in the patient, and her mother with a relatively lower sequencing depth than her father. Although CNV sequencing showed no evidence of a microdeletion, subsequent qPCR investigation showed a deletion containing the *CHKB* gene. For patient 2, segmental paternal UPD in chromosome 22 was confirmed by comparing parental genotyping with SNPs and polymorphic microsatellite markers, implying that the same pathogenic variant on both alleles of chromosome 22 was inherited only from his father.

From 2011 to 2022, 49 megaconial CMD patients with compound heterozygous and homozygous *CHKB* gene variants, from 45 families, were reported. The phenotypic spectrum of *CHKB* mutations ranges from a congenital muscular dystrophy with intellectual disability to a later-onset non-progressive muscular weakness with normal cognition (Brady et al., 2016). The clinical findings of 35 patients have been previously reported by Chan et al. (2020) and the clinical manifestations of the two children in this study were consistent with previous reports. Except a patient diagnosed with coexistence of Megaconial CMD and Cystinuria (Surucu et al., 2022), a total of 50 patients including our two cases are further summarized.

The prognosis of megaconial CMD seems up to cardiac manifestation, and the median age at the last follow-up was 10 years (range: 2–40 years). Six patients died early due to infection or dilated cardiomyopathy (range: 2–23 years, the median age of death, 7.5 years) (Haliloglu et al., 2015; Mitsuhashi et al., 2011; Quinlivan et al., 2013; Ríos et al., 2012). After strenuous exercise, patients with megaconial CMD are prone to fatigue, myalgia, and rhabdomyolysis. Like a mitochondrial disease, seven children showed motor regression or deterioration of

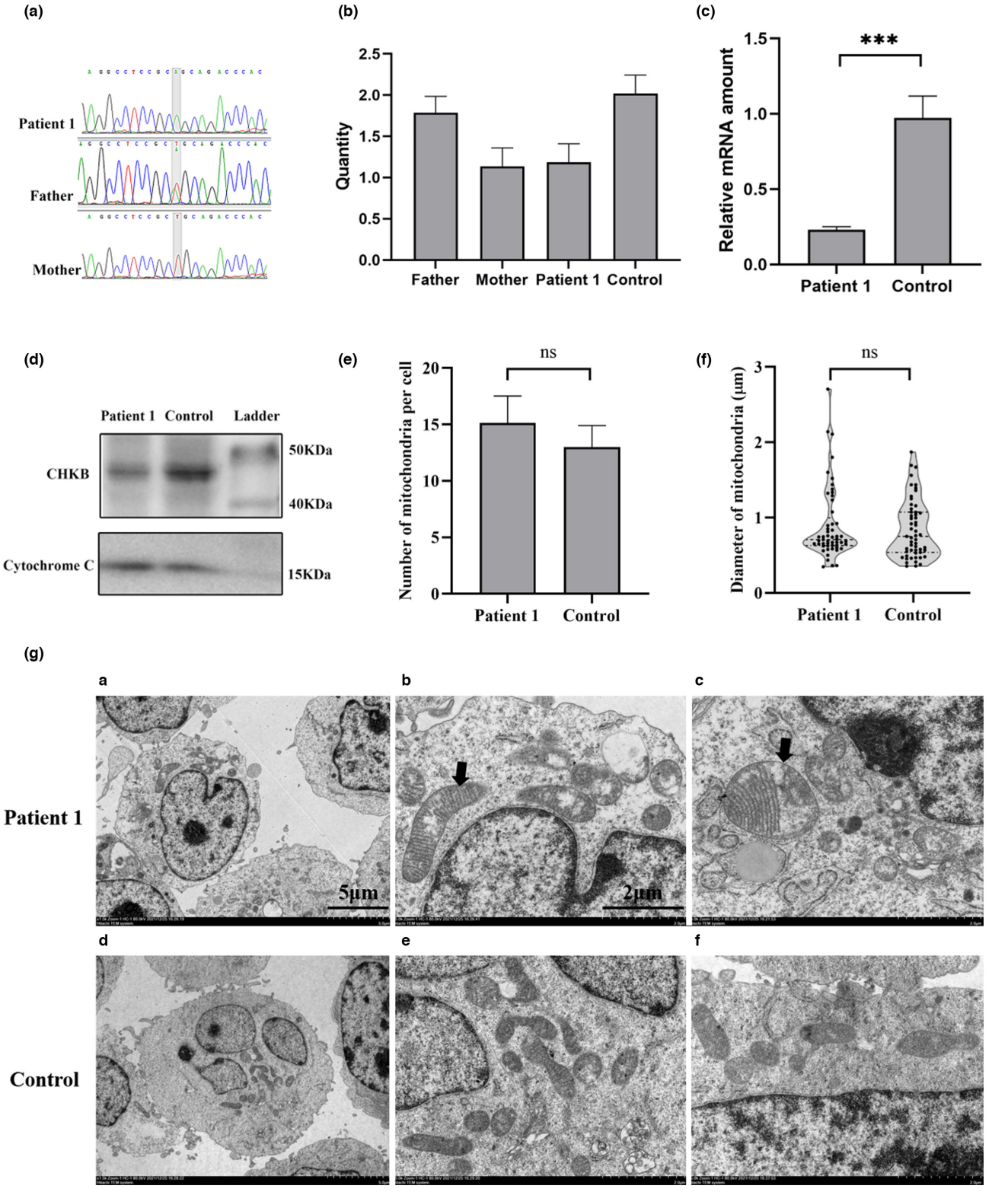

FIGURE 1 (a) The electropherograms of patients 1; (b) qPCR analysis of the exon deletion in patient 1, her parents, and the healthy control; (c) Quantitative analysis of mRNA in CHKB using β-Actin as an internal control. (d) Western blot analysis of CHKB in immortalized lymphocytes using Cytochrome C as an internal control. (e) The number of mitochondria per cell in immortalized lymphocytes from patient 1 and healthy control. (f) The length of the mitochondrial axis in immortalized lymphocytes from patient 1 ($n = 53$) and healthy control ($n = 55$). (g) Typical mitochondrial size and morphology were evaluated by electron microscopy. (a and d) original magnification: ×1.5 K, excessive accumulations of mitochondria were not seen; (b and c) original magnification: ×5 K; large mitochondria indicated by arrows in immortalized lymphoblastoid cells of patient 1, and a more bright and swollen aspect with disorganized and ruptured-like cristae. (e and f) original magnification: ×5 K; mitochondria of healthy control.

TABLE 1 Detailed whole exome sequencing data.

	Mean coverage						Alt/All		
Patients	**Proband**	**Father**	**Mother**	**Variant**	**Location**	**gnomAD MAF**	**Proband**	**Father**	**Mother**
Patient 1	117.17	127.07	139.04	c.225-2A>T	Chr22:50582359	—	67/67	44/97	0/59
Patient 2	162.65	132.8	145.68	c.701C>T	Chr22:50580393	0.00001591	231/231	0/261	105/239

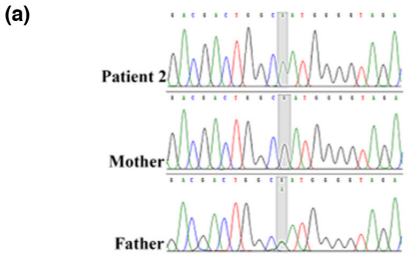

(b)

Location	Name	Father		Mother		Patient 2	
chr22:46461956	rs4823818	1	1	0	0	1	1
chr22:46462445	rs28360648	1	1	0	0	1	1
chr22:46462646-46462649	rs10541493	0	2	1	2	0	0
chr22:46462790	rs5768788	0	1	1	1	0	0
chr22:49919154-49919170	rs145212257	0	1	0	0	1	1
chr22:50447465-50447466	rs56853707	0	1	1	1	0	0
chr22:50474966-50474968	rs373485644	1	1	1	1	1	1
chr22:50487004-50487006	rs145924823.	0	1	0	0	1	1
chr22:50575569	rs1557502	1	1	1	1	1	1
chr22:50576781	rs140515	1	1	1	1	1	1
chr22:50577128	rs3752393	1	1	1	1	1	1
chr22:50577245	rs3213446	1	1	0	1	1	1
chr22:50578780	rs10627369	1	1	0	1	1	1
chr22:50578867	rs8137478	1	1	0	1	1	1
chr22:50578924	rs5770917	1	1	0	1	1	1
chr22:50578965	rs3180872	1	1	0	1	1	1
chr22:50579047	rs1056964	1	1	0	1	1	1
chr22:50579085	rs17001634	0	0	0	1	0	0
chr22:50579284	rs762677	1	1	0	1	1	1
chr22:50579365	rs762676	1	1	0	1	1	1
chr22:50580393	rs764209313	0	1	0	0	1	1
chr22:50580482	rs2269382	1	1	0	1	1	1
chr22:50581186	rs62239538	0	0	0	1	0	0
chr22:50581640	rs2269381	1	1	0	1	1	1
chr22:50582239	rs86337	1	1	0	1	1	1
chr22:50582836-50582855	rs144647670	1	1	0	1	1	1
chr22:50583150	rs131757	1	1	1	1	1	1
chr22:50583252	rs186951258	1	1	0	0	1	1
chr22:50595411	rs7284429	1	1	1	1	1	1

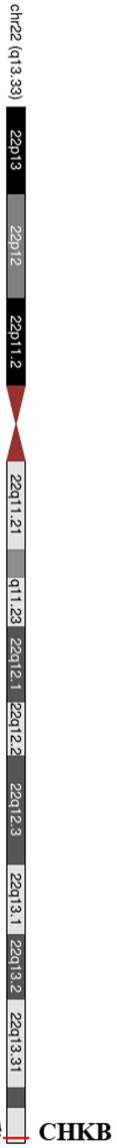

FIGURE 2 (a) The electropherograms of patients 1; (b) Partial detailed information on the SNPs near CHKB are also shown. The region in the yellow background represented the overlapping with CHKB. The genotyping in the red font indicated the allele that was inherited from her father.

cardiac function after fatigue, infection, or surgery (Brady et al., 2016).

The CK levels in megaconial CMD ranged from normal to 9000 U/L (40 times the upper limit), and the CK increase in most patients (45/48) was less than ten times. The CK level can be used to distinguish megaconial CMD from Duchenne muscular dystrophy, as the CK level of the latter is usually significantly increased 10–20-fold after birth and peaking at 50–100 fold by the age of 5 (Bushby et al., 2010). Rhabdomyolysis was observed in a patient

after exercise, with CK increasing to 20,000 U/L (Brady et al., 2016). In addition, electromyography suggests muscle involvement, and muscle MRI shows that muscle tissue is replaced by fat, which are important indicators of megaconial CMD. Patient 2 showed a mild phenotype, as reported previously (De Fuenmayor-Fernández et al., 2016), with normal muscle MRI at 14 years of age.

A total of 44 children underwent muscle biopsies, and enlarged mitochondria were found by electron microscopy. The activity of respiratory chain enzymes in muscle mitochondria varied between patients showing single or multiple complex enzyme deficiencies (Quinlivan et al., 2013; Ríos et al., 2012), even normal (De Fuenmayor-Fernández et al., 2016). Therefore, respiratory chain enzyme activity is not a specific diagnostic marker. Muscle biopsy is most appropriate to confirm the diagnosis of megaconial CMD. In this study, the parents refused a muscle biopsy, so we attempted to use immortalized lymphocytes of patient 1 to detect mitochondrial pathological changes. Enlarged mitochondria were observed in lymphocytes using electron microscopy, which provided another possibility for detecting giant mitochondria. However, it is currently only available in a research lab. Because there is not an exact definition for "abnormal giant mitochondria", the percentage of cells with "abnormal giant mitochondria" is difficult to be confirmed, especially there are only a limited number of cells and mitochondria in this study. A larger sample size is needed to confirm the standard for "abnormal giant mitochondria".

Nonetheless, molecular genetic analysis is an alternative to muscle biopsy if the clinical phenotypes support a CMD diagnosis. In our case, the proband was suspected of having CMD owing to developmental delay/intellectual disability, muscle weakness, high serum CK levels, and electromyography abnormalities. The molecular genetic analysis identified homozygous *CHKB* mutations. A total of 35 different mutations were identified (Figure 3), of which approximately two-thirds represented presumed loss-of-function variants (seven were nonsense, seven were frameshift mutations, five were splice-site mutations, and two were deletion), while one-third were missense changes which clustered in different exons. Recombinant missense CHKB proteins, including p.Asn241Ser, p.Glu283Lys, and p.Arg377Leu markedly decreased choline kinase activities, indicating that these mutations were loss-of-function (Mitsuhashi et al., 2011). The c.225-2A>T is classified as "possibly pathogenic" according to the American Academy of Medical Genetics and Genomics (ACMG) (Richards et al., 2015). As a loss-of-function variant, c.225-2A>T caused significant decreases of *CHKB* mRNA and protein expression, which is consistent with the pathogenic mechanism of loss-of-function in the *CHKB* gene. The second variant, c.701C>T, in patient 2, has been reported in a Bulgarian patient with a similar phenotype with enlarged mitochondria in the muscle biopsy (De Fuenmayor-Fernández et al., 2016). According to ACMG classification guidelines, the c.701C>T variant is classified as "possibly pathogenic".

Most patients (43/51) had homozygous variants. Since true causative-gene homozygous variants are more likely to occur in consanguineous families, consanguinity was reported in 20 patients with homozygosity though their parents were not tested. The genetic presentation of the other 23 patients not from consanguineous families was summarize in Table 2, and a flow diagram depicted various reasons leading to homozygosity, which may guide to explore potential etiology (Figure 4). At first, the parental DNAs should be analyzed to assess homozygosity and biological relationship. Eight patients from non-consanguineous families harbored homozygosity inherited from their parents, which was the largest part leading to homozygosity in non-consanguineous

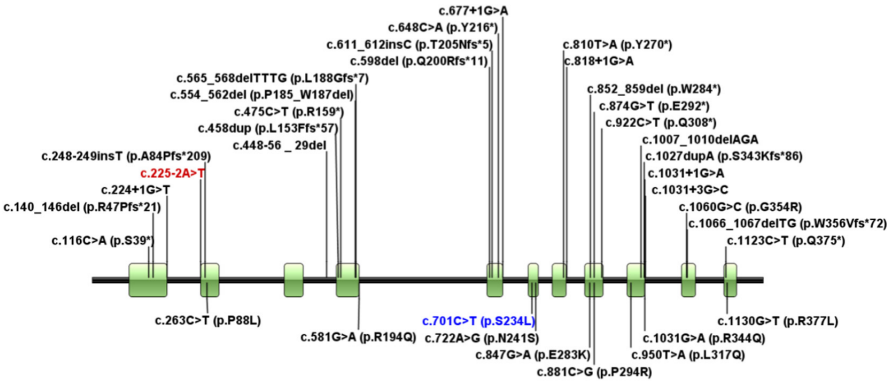

FIGURE 3 Disease-causing mutations in the *CHKB* gene. Diagram of *CHKB* gene indicating previously reported and recently identified patient mutations. Loss-of-function variants (nonsense mutation, frameshift mutation, splice-site mutation, and deletion mutation) are presented above, and missense variants are presented below. The patient 1 variant is highlighted in red (another variant of large deletion is not shown), and the patient 2 variant is in blue.

TABLE 2 Summary of the genetic presentation of the patients with homozygosity (not including those from consanguineous families).

Patients	cDNA	Consequence	Paternal	Maternal	Reference
1	c.1123C>T	p.Gln375Ter	NA	NA	Bardhan et al. (2021)
2	c.1031+1G>A	—	NA	NA	Mitsuhashi et al. (2011), Haliloglu et al. (2015)
3	c.1031+1G>A	—	NA	NA	Kutluk et al. (2020)
4	c.1027dupA	p.Ser343LysfsTer86	NA	NA	Bardhan et al. (2021)
5[a]	c.1007_1010delAGA	—	wt	het	Haliloglu et al. (2015)
6	c.874G>T	p.Glu292Ter	NA	NA	Ríos et al. (2012)
7	c.810T>A	p.Tyr270Ter	het	het	Castro-Gago et al. (2014)
8	c.810T>A	p.Tyr270Ter	NA	NA	Castro-Gago et al. (2016)
9	c.810T>A	p.Tyr270Ter	NA	NA	Mitsuhashi et al. (2011)
10	c.810T>A	p.Tyr270Ter	NA	het	Mitsuhashi et al. (2011)
11[a]	c.722A>G	p.Asn241Ser	het	wt	Quinlivan et al. (2013)
12	c.722A>G	p.Asn241Ser	NA	NA	De Goede et al. (2016)
13	c.701C>T	p.Ser234Leu	NA	het	De Fuenmayor-Fernández et al. (2016)
14*	c.701C>T	p.Ser234Leu	het	NA	This study
15	c.677+1G>A	—	NA	NA	Mitsuhashi et al. (2011), Haliloglu et al. (2015)
16	c.581G>A	p.Arg194Gln	NA	NA	Mitsuhashi and Nishino (2013)
17	c.581G>A	p.Arg194Gln	het	het	Bardhan et al. (2021)
18	c.598del	p.Gln200Argfs*11	het	het	Chan et al. (2020)
19	c.598del	p.Gln200Argfs*11	het	het	Chan et al. (2020)
20	c.565_568delTTTG	p.Leu188Glyfr*7	het	het	Marchet et al. (2019)
21	c.565_568delTTTG	p.Leu188Glyfr*7	het	het	Marchet et al. (2019)
22	c.248-249insT	p.Arg84Profs*209	het	het	Vanlander et al. (2016)
23[b]	c.225-2A>T	—	het	wt	This study

Abbreviations: NA, not available; wt, wild type.

[a]Segmental paternal UPD.

[b]Overlapping exon deletion.

families. Second, as showed in flow diagram (Figure 4), a total of four patients with homozygous variants showed that only a single parent harbored the same heterozygous variant, including two previously reported patients (Haliloglu et al., 2015; Quinlivan et al., 2013). The potential molecular etiologies, such as an overlapping exon deletion or UPD, which accounted a larger proportion compared with a germline mosaicism or de novo variant, should be further analyzed. Because germline mosaicism is difficult to be diagnosed due to germ cells that were not easily obtained, it rarely occurred that a de novo variant is consistent with the mutant allele. Moreover, UPD is generally thought to occur at a rate of 1:3500 live births (Robinson, 2000). In this situation, overlapping deletion and UPD analyses will be easy but effective approaches to assess the presumed homozygosity. In nine non-consanguineous families, whose co-segregation was not confirmed due to unavailable parent test results, the overlapping deletion and UPD may account for a proportion according to current data.

UPD can be ascertained through analysis of SNPs distribution from trio genotype data in the context of exome or genome sequencing, which may not always be provided in variant analysis reports. WES has been proven successful for the detection of clinically relevant point mutations and small insertion-deletions exome wide (de Ligt et al., 2013); however, in present study, a heterozygous deletion of *CHKB* remained undetected by the combination of trio WES and CNV sequencing. The real-time qPCR with low cost and labor is widely used in measuring quantitative information about the exact copy number of the gene. We recommend qPCR as a routine clinical setting and the preferred method to confirm the deletion. Additional analyses besides genetic reports, such as qPCR, SNPs and polymorphic microsatellite markers distribution are necessary to reveal deletion and UPD.

In conclusion, we identified a novel splice site variant and observed enlarged mitochondria in immortalized lymphocytes, providing a possibility to detect giant mitochondria in other cells when muscle was not available.

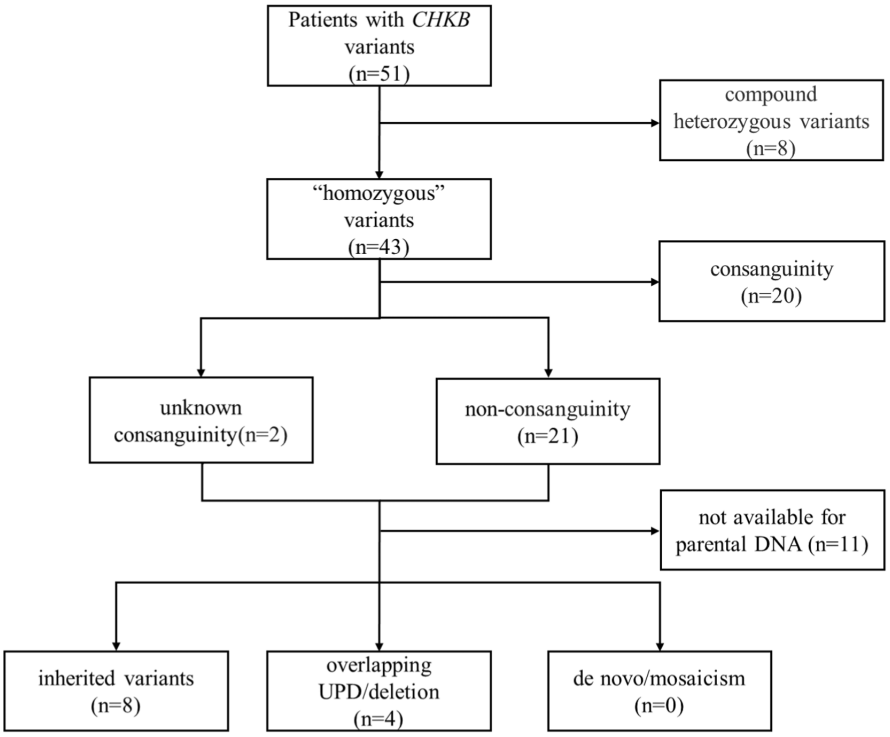

FIGURE 4 The flow diagram to depict various reasons leading to homozygosity.

Since homozygosity accounted for a large percentage in megaconial CMD, a comprehensive genetic analysis was necessary for avoiding excessive diagnosis of homozygosity. Patients were identified with "presumed homozygous" variants, whereas only a single parent was found to harbor the same heterozygous variant by Sanger sequencing. The potential molecular etiologies, such as an overlapping exon deletion and UPD, should be suspected and analyzed.

AUTHOR CONTRIBUTIONS

Tenghui Wu drafted the manuscript and performed the experiments. Ciliu Zhang, Fang He and Fei Yin performed patient clinical management and analyzed the clinical data. Li Yang analyzed the electron microscopy data. Jing Peng supervised the work and designed the research.

ACKNOWLEDGMENTS

We thank the patients and their families for their participation in the study. We thank Tang Guizhi (Hunan Key Laboratory of Medical Genetics, Central South University, China) for helping immortalize lymphocytes. We thank CIPHER GENE for helping analysis of whole exome sequencing.

FUNDING INFORMATION

This work was supported by the National Natural Science Foundation of China (NO. 82071462).

CONFLICT OF INTEREST STATEMENT

None of the authors have any conflicts of interest to disclose.

ETHICS

This study was approved by the Ethics Committee of Xiangya Hospital of Central South University, China (Human study/protocol #201605585).

CONSENT TO PARTICIPATE

Informed consent was obtained from the guardian of patient.

DATA AVAILABILITY STATEMENT

Data available within the article or its supplementary materials.

ORCID

Li Yang https://orcid.org/0000-0002-3228-2140
Jing Peng https://orcid.org/0000-0002-7752-6962

REFERENCES

Bardhan, M., Polavarapu, K., Bevinahalli, N. N., Veeramani, P. K., Anjanappa, R. M., Arunachal, G., Shingavi, L., Vengalil, S., Nashi, S., Chawla, T., Nagabushana, D., Mohan, D., Horvath, R., Nishino, I., & Atchayaram, N. (2021). Megaconial congenital muscular dystrophy secondary to novel CHKB mutations resemble atypical Rett syndrome. *Journal of Human Genetics*, *66*(8), 813–823.

Brady, L., Giri, M., Provias, J., Hoffman, E., & Tarnopolsky, M. (2016). Proximal myopathy with focal depletion of mitochondria and megaconial congenital muscular dystrophy are allelic conditions caused by mutations in CHKB. *Neuromuscular Disorders*, *2*(26), 160–164.

Bushby, K., Finkel, R., Birnkrant, D. J., Case, L. E., Clemens, P. R., Cripe, L., Kaul, A., Kinnett, K., McDonald, C., Pandya, S., &

Poysky, J. (2010). Diagnosis and management of Duchenne muscular dystrophy, part 1: Diagnosis, and pharmacological and psychosocial management. *The Lancet Neurology*, *1*(9), 77–93.

Castro-Gago, M., Dacruz-Alvarez, D., Pintos-Martínez, E., Beiras-Iglesias, A., Arenas, J., Martín, M. Á., & Martínez-Azorín, F. (2016). Congenital neurogenic muscular atrophy in megaconial myopathy due to a mutation in CHKB gene. *Brain Dev*, *1*(38), 167–172.

Castro-Gago, M., Dacruz-Alvarez, D., Pintos-Martínez, E., Beiras-Iglesias, A., Delmiro, A., Arenas, J., Martín, M. Á., & Martínez-Azorín, F. (2014). Exome sequencing identifies a CHKB mutation in Spanish patient with megaconial congenital muscular dystrophy and mtDNA depletion. *European Journal of Paediatric Neurology*, *6*(18), 796–800.

Chan, S. H., Ho, R. S., Khong, P. L., Chung, B. H., Tsang, M. H., Mullin, H. C., Yeung, M. C., Chan, A. O., & Fung, C. W. (2020). Megaconial congenital muscular dystrophy: Same novel homozygous mutation in CHKB gene in two unrelated Chinese patients. *Neuromuscular Disorders*, *1*(30), 47–53.

Chomczynski, P., & Sacchi, N. (2006). The single-step method of RNA isolation by acid guanidinium thiocyanate-phenol-chloroform extraction: Twenty-something years on. *Nature Protocols*, *2*(1), 581–585.

De Fuenmayor-Fernández, D. L. H. C., Domínguez-González, C., Gonzalo-Martínez, J. F., Esteban-Pérez, J., Fernández-Marmiesse, A., Arenas, J., Martín, M. A., & Hernández-Laín, A. (2016). A milder phenotype of megaconial congenital muscular dystrophy due to a novel CHKB mutation. *Muscle & Nerve*, *4*(54), 806–808.

De Goede, C., Oh, T., Joseph, J., Muntoni, F., Sewry, C., & Phadke, R. (2016). Choline kinase beta-related muscular dystrophy, appearance of muscle involvement on magnetic resonance imaging. *Pediatric Neurology*, *54*, 49–54.

de Ligt, J., Boone, P. M., Pfundt, R., Vissers, L. E., Richmond, T., Geoghegan, J., O'Moore, K., de Leeuw, N., Shaw, C., Brunner, H. G., & Lupski, J. R. (2013). Detection of clinically relevant copy number variants with whole-exome sequencing. *Human Mutation*, *10*(34), 1439–1448.

Haliloglu, G., Talim, B., Sel, C. G., & Topaloglu, H. (2015). Clinical characteristics of megaconial congenital muscular dystrophy due to choline kinase beta gene defects in a series of 15 patients. *Journal of Inherited Metabolic Disease*, *6*(38), 1099–1108.

Ishidate, K. (1997). Choline/ethanolamine kinase from mammalian tissues. *Biochimica et Biophysica Acta*, *1-2*(1348), 70–78.

Kutluk, G., Kadem, N., Bektas, O., & Eroglu, H. N. (2020). A rare cause of autism Spectrum disorder: Megaconial muscular dystrophy. *Annals of Indian Academy of Neurology*, *5*(23), 694–696.

Marchet, S., Invernizzi, F., Blasevich, F., Bruno, V., Dusi, S., Venco, P., Fiorillo, C., Baranello, G., Pallotti, F., Lamantea, E., Mora, M., Tiranti, V., & Lamperti, C. (2019). Alteration of mitochondrial membrane inner potential in three Italian patients with megaconial congenital muscular dystrophy carrying new mutations in CHKB gene. *Mitochondrion*, *47*, 24–29.

Mitsuhashi, S., & Nishino, I. (2013). Megaconial congenital muscular dystrophy due to loss-of-function mutations in choline kinase *β*. *Current Opinion in Neurology*, *5*(26), 536–543.

Mitsuhashi, S., Ohkuma, A., Talim, B., Karahashi, M., Koumura, T., Aoyama, C., Kurihara, M., Quinlivan, R., Sewry, C., Mitsuhashi, H., & Goto, K. (2011). A congenital muscular dystrophy with mitochondrial structural abnormalities caused by defective de novo phosphatidylcholine biosynthesis. *American Journal of Human Genetics*, *6*(88), 845–851.

Quinlivan, R., Mitsuahashi, S., Sewry, C., Cirak, S., Aoyama, C., Mooore, D., Abbs, S., Robb, S., Newton, T., Moss, C., & Birchall, D. (2013). Muscular dystrophy with large mitochondria associated with mutations in the CHKB gene in three British patients: Extending the clinical and pathological phenotype. *Neuromuscular Disorders*, *7*(23), 549–556.

Richards, S., Aziz, N., Bale, S., Bick, D., Das, S., Gastier-Foster, J., Grody, W. W., Hegde, M., Lyon, E., Spector, E., & Voelkerding, K. (2015). Standards and guidelines for the interpretation of sequence variants: A joint consensus recommendation of the American College of Medical Genetics and Genomics and the Association for Molecular Pathology. *Genetics in Medicine*, *5*(17), 405–424.

Ríos, P. G., Kalra, A. A., Wilson, J. D., Tanji, K., Akman, H. O., Gómez, E. A., Schon, E. A., & DiMauro, S. (2012). Congenital megaconial myopathy due to a novel defect in the choline kinase beta gene. *Archives of Neurology*, *5*(69), 657–661.

Robinson, W. P. (2000). Mechanisms leading to uniparental disomy and their clinical consequences. *BioEssays*, *5*(22), 452–459.

Surucu, K. I., Oncul, U., Kose, E., Turan, H. M., Ceylan, A. C., & Eminoglu, F. T. (2022). Coexistence of megaconial congenital muscular dystrophy and cystinuria: Mimicking hypotonia-cystinuria syndrome. *Mol Syndromol*, *3*(13), 240–245.

Vanlander, A. V., Muiño, M. L., Panzer, J., Deconinck, T., Smet, J., Seneca, S., Van Dorpe, J., Ferdinande, L., Ceuterick-de Groote, C., De Jonghe, P., & Van Coster, R. (2016). Megaconial muscular dystrophy caused by mitochondrial membrane homeostasis defect, new insights from skeletal and heart muscle analyses. *Mitochondrion*, *27*, 32–38.

Wu, T., Mao, L., Chen, C., Yin, F., & Peng, J. (2022). A novel homozygous missense mutation in the FASTKD2 gene leads to Lennox-Gastaut syndrome. *Journal of Human Genetics*, *10*(67), 589–594.

How to cite this article: Wu, T., Zhang, C., He, F., Yang, L., Yin, F., & Peng, J. (2023). Large heterozygous deletion and uniparental disomy masquerading as homozygosity in *CHKB* gene. *Molecular Genetics & Genomic Medicine*, *11*, e2162. https://doi.org/10.1002/mgg3.2162